Optical Feeder Links for Multi-GEO Multi-OGS Networks: Nodes Analysis to Maximize Connectivity Under Dynamic Cloud Coverage

Robert T. Schwarz *Member, IEEE*, Hung Le Son *Graduate Student Member, IEEE*, Marcus T. Knopp, and Andreas Knopp *Senior Member, IEEE*

***Abstract*—Optical feeder links (OFLs) to geostationary orbit (GEO) satellites present a promising solution to significantly enhance the throughput of satellite systems, especially those with high data rate demands, such as satellite constellations. However, cloud coverage substantially increases the likelihood of link outages, thereby reducing the availability of optical ground stations (OGSs) and limiting the number of possible connections between the GEO and OGS networks. This paper introduces a maxflow-based OFL planning concept aimed at maximizing the number of ground-to-GEO OFL connections under the influence of dynamic cloud coverage. Various network scenarios are considered—featuring different numbers of satellites, OGSs, and varying degrees of visibility correlation—to optimize the network design. The average system capacity is estimated through Monte Carlo simulations, while system availability is stochastically evaluated. Simulation results show that network capacity depends mainly on the number of GEO satellites, while visibility correlation has a strong impact on availability. Furthermore, the simulations reveal that even under a high correlation of visibility and a high probability of link outages, only a small number of additional OGSs are sufficient to achieve the theoretical upper bound of capacity. These insights can contribute to cost-efficient network design by identifying the optimal number of GEO satellites and OGSs required to meet operational demands.**

***Index Terms*—Optical feeder links, network planning, link availability, cloud statistics, free-space optical communications, maximum flow problem.**

I. Introduction

Satellite constellations have emerged as a transformative solution for global Internet access from space, introducing unprecedented possibilities for connectivity in the Fifth Generation of Mobile Technology (5G) framework, as recognized by the 3rd Generation Partnership Project (3GPP) Release 17. Driven by increasing user demand for data, the throughput of these constellations has grown exponentially, largely due to the high data transfer rates enabled by intersatellite links (ISLs). However, a critical challenge persists in meeting the data rate requirements in the terabit-per-second ($\mathrm{Tbit/s}$) range through feeder links. Traditionally, radio frequency (RF) links in the Ku-band (12-14 GHz) and the Ka-band (20-30 GHz) are utilized for these connections. Each ground station can typically allocate 1-2 GHz of bandwidth [1], supporting merely data rates of a few $\mathrm{Gbit/s}$ per ground station. Thus, the RF feeder link in those frequency bands alone is no longer sufficient to satisfy the data-rate demand on the order of $\mathrm{Tbit/s}$ in future satellite constellations.

Most current optical terminals, constrained by narrow laser beams, limit satellites to single-optical ground station (OGS) connections at a time. Given the high costs of geostationary orbit (GEO) satellites and OGS infrastructure, with only several OGSs constructed and operational globally as of the time of writing [2]–[4], network architectures must optimize the number of satellite-to-OGS connections, while minimizing the probability of network outages and handling the dynamic nature of the atmosphere. Existing studies often focus on optical feeder link (OFL) in single-satellite scenarios, leaving satellite constellations underexplored. Furthermore, in our previous study, we demonstrated that satellites at different angular positions experience a certain diversity of visibility from an OGS [5]. Thus, satellite multiplexing can be utilized to improve the availability of each individual OGS, further reducing the required number of OGSs in an OGS network to achieve the same system availability. Future low earth orbit (LEO) satellite constellations are also planned to be capable of establishing direct-to-earth (DTE) optical links. Given that thousands of satellites are in LEO orbits, each OGS should select the best satellites among those within its field of regard (FOR). An efficient short-term link planning framework is therefore critical.

OGS network topology has been extensively studied in the literature. The network design is primarily based on cloud obstruction statistics, which constitute the main reason for system outages of OFLs. This data is conventionally analyzed using cloud climatology images from Earth observation satellites. In 2006, Link et al. [6], [7] developed a high-resolution multispectral cloud climatology model to enhance the strategic placement of ground stations across the United States. In Europe, Benarroch et. al. studied the spatial properties, distribution, and correlation of cloud coverage in [8], [9]. Subsequently, Moll et. al. [10] analyzed the availability of links using data from the European Cloud Climatology (ECC). Lacoste et. al. [11] also contributed to this field in 2011 by conducting a meteorological study on cloud statistics to identify optimal locations for optical ground stations (OGSs)

R. T. Schwarz is with the Munich Center for Space Communications, University of the Bundeswehr Munich, Neubiberg, Germany

H. Le Son is with the Munich Center for Space Communications, University of the Bundeswehr Munich, Neubiberg, Germany

Marcus T. Knopp is with the Munich Center for Space Communications, University of the Bundeswehr Munich, Neubiberg, Germany

A. Knopp is with the Munich Center for Space Communications, University of the Bundeswehr Munich, Neubiberg, Germany

Manuscript received April 1, 2025, revised November 4, 2025.

in Northwestern Europe. Building upon satellite-based cloud coverage assessments, Fuchs et. al. later proposed a comprehensive OGS network spanning national (Germany), European, and international scales [12], [13]. Poulenard et. al. introduced a GEO-to-ground network with optimized costs that exploits existing high-data-rate fiber links [14].

Several studies have shown that there are notable discrepancies between cloud fraction detection results from satellite images and all-sky imager (ASI) measurements [15]. Therefore, the space-ground OFL network topology should also consider the perspective of OGSs. In Japan, the National Institute of Information and Communications Technology deployed a ground-based environmental-data collection testbed for site-diversity implementation across 10 locations [16]. To further enhance the accuracy of cloud obstruction assessment, ground-based cloud detection systems using ASI that were originally developed in the solar energy industry can be repurposed for this application [17]. Compared to satellite imagery, a ground-based cloud monitoring and prediction system can provide significantly higher temporal (1 minute) and spatial (better than 0.1°) resolution [18]. This high resolution is critical for agile and reactive short-term link planning in the OFL network to effectively handle cloud dynamics.

Fürbacher et. al. introduced a prototype of a link planning system in [19]. In overbooked OGS networks, Fürbacher's work included user fairness as a scheduling criterion. However, in future DTE-free-space optical communication (FSOC)-capable satellite constellations, in which traffic data can be balanced through ISL and fiber links, the capacity sum of all OFLs is a more important measure for evaluating network performance. Liu et al. proposed a link management algorithm in space-ground integrated optical networks (SGIONs), considering the trade-off between throughput and dynamics [20].

In this context, we introduce a novel planning approach for OFLs within a multiple-satellite multiple-OGSs network to maximize simultaneous satellite-OGS connections under dynamic link availabilities. Among multiple factors in the Earth's atmosphere that can influence the data rate of an OFL, including turbulence-induced fading and elevation-dependent atmospheric attenuation [21], we restrict our investigation in this study to cloud obstruction. Based on the results of applying the proposed approach, we analyze the ground-to-GEO OFL network's performance in terms of capacity and outages in various scenarios. Key variables include the number of GEO satellites, OGSs, and correlations in visibility between different line-of-sight (LOS) propagation paths.

The main contributions of this paper are the following:

- We formulate the problem of optimizing the number of connections as a maximum flow problem. The solution for each visibility matrix represents the network topology of optimal capacity.
- We evaluate the influence of factors including the number of communication nodes (satellites and OGSs) and the correlation in visibility between LOS paths when the proposed link planning approach is applied.
- We provide insights into optimal network architectures that balance capacity, reliability, and the number of required communication nodes.

The remainder of this paper is organized as follows: In Section II, we describe the investigated scenario of OFLs in satellite constellations and formulate the connection optimization problem. In Section III, we detail our methodology for assessing the average capacity and reliability of the network. In Section IV, we present the simulation results and discuss the optimal network architecture. Finally, in Section V, we conclude the paper and discuss future work.

II. Scenario Description

A. Multi-GEO Multi-OGS Network Model

We consider a OFL network consisting of N GEO satellites and M OGSs, as illustrated in Fig. 1. The satellites are interconnected via ISLs, while the OGSs are linked through the existing terrestrial fiber network. ISLs and the fiber network are assumed to be highly reliable, enabling efficient load balancing within the inter-satellite and inter-OGS domains. In contrast, link interruptions and signal degradations occur exclusively along the optical LOS paths due to cloud blockage, atmospheric attenuation, and turbulence. With support from the cloud monitoring system, we assume cloud prediction accuracy to be sufficient for link planning purposes. Several recent studies have demonstrated the feasibility of short-term (intra-hour) cloud forecasting [22], [23]. The elevation-dependent link budget can also be accurately estimated from satellite orbital positions, as shown in [24].

In this study, we focus solely on the impact of cloud coverage on network performance, thereby neglecting elevation-dependent factors like atmospheric attenuation and turbulence. In real-world implementations they will certainly affect link outage probability. However, concrete system parameters such as transmission power, reception sensitivity, antenna gains and losses are required to be able to calculate link budgets accurately. In real system designs a link margin of -6 dB on the average received power attributed to atmospheric effects is usually sufficient to account for those effects. Since the current work sets its focus on the GEO-to-ground connectivity rather than on a throughput assessment, detailed link budget analyses are deferred for future work.

Given that the median duration of cloud-free and cloud-covered durations ranges between 1.5 and 2 minutes found in our previous work [5], the link planning frequency of a similar order should be employed. For each time frame of duration $\Delta t \approx 2\,\mathrm{min}$, we assume static cloud coverage across all LOS paths. The visibility of satellites to OGSs can be described in a visibility matrix given by

$$\mathbf{V}_i = \begin{bmatrix} v_{11} & v_{12} & \cdots & v_{1N} \\ v_{21} & v_{22} & \cdots & v_{2N} \\ \vdots & \vdots & \ddots & \vdots \\ v_{M1} & v_{M2} & \cdots & v_{MN} \end{bmatrix}, \tag{1}$$

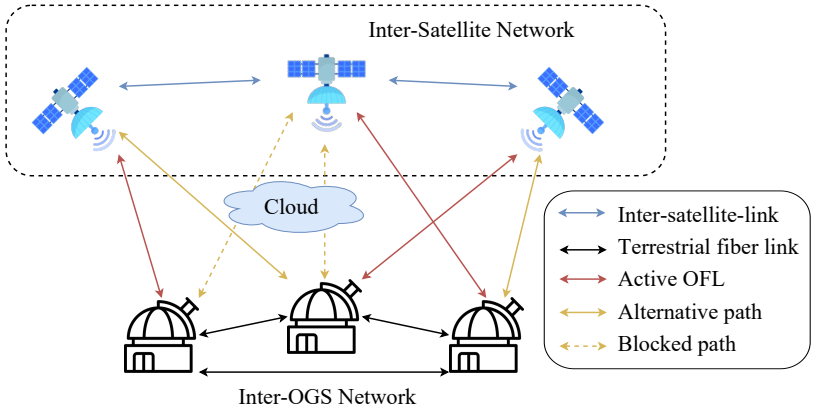

Fig. 1. Illustrative multi-GEO, multi-OGS network with $N = 3$ and $M = 3$. The three red bidirectional solid lines indicate unobstructed LOS paths corresponding to established OFLs, whereas the yellow solid lines denote two alternative OFL candidates. The link-planning objective is to form a node-disjoint OFL topology that maximizes the space-to-ground throughput.

where v_{mn} represents the link availability between the n-th satellite and the m-th OGS. For simplicity, we model the visibility between each satellite–OGS pair as a binary variable, i.e., $v_{mn} \in \{0, 1\}$. Based on this short-term cloud forecast, the link planner can select an optimized topology for each time frame.

Because OGSs are typically separated by hundreds of kilometers to mitigate correlated weather, the visibility of a given satellite to different OGSs can be treated as statistically independent. In contrast, a single weather event can obstruct visibility across an entire region. Therefore, the visibility of multiple satellites to the same OGS is correlated. Empirical measurements based on data from all-sky cameras indicate that the correlation of the visibility of the satellites to the same OGS can reach $80\,\%$ [5]. We model the visibility matrix as binary with a row-wise correlation among variables. Throughout the remainder of this work, the visibility correlation indicates the correlation in the paths from satellites to the same OGS, that is, elements in the same rows of the visibility matrix.

Due to the narrow divergence of the laser beam, an optical aperture on a satellite can establish a link with only one OGS at a time. To minimize design complexity and cost, we assume that each satellite is equipped with a single aperture for the DTE connection. Under this assumption, the link management system is responsible for selecting the most suitable OGS for each satellite, with the objective of maximizing the number of simultaneous satellite-to-OGS connections. Since all visible LOS paths are assigned an equal capacity of one unit, the selection process can be formulated as a maximum-flow problem. Consider a directed graph $G = (V, E)$, where s and t denote the source and sink vertices, respectively. The edge set E includes visible paths e_{mn} between the n-th satellite and the m-th OGS, each associated with a capacity v_{mn}. The objective is to determine the maximum number of vertex-disjoint paths from s to t, corresponding to feasible satellite-OGS assignments. After reaching a satellite vertex n from the source s, the algorithm must select one of the available edges e_{mn}, as each preceding edge can carry only a unit flow. Consequently, the maximum flow from the source s to the sink t directly represents the maximum number of satellites that can be connected simultaneously to OGSs. The problem is illustrated in a maxflow graph in Fig. 2. In this work, the maximum flow is calculated using the Boykov–Kolmogorov algorithm, as introduced in [25].

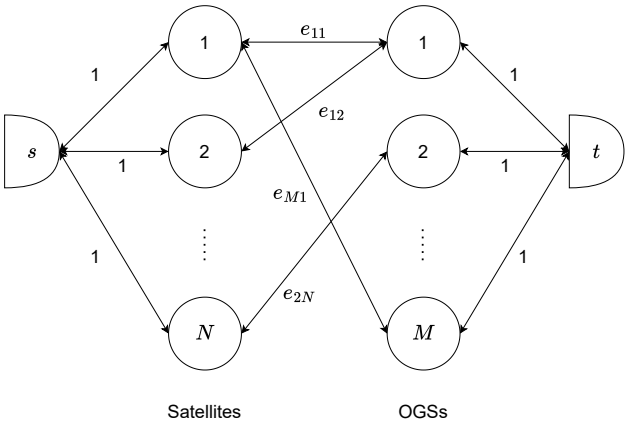

Fig. 2. Formulation of the maximum-number-of-connections problem as a maxflow graph. Here, each satellite is limited to connect to a single OGS at a time. An edge weight of $e_{mn} = 1$ indicates a visible LOS path that can be selected for topology formation.

B. Ground-based Cloud Cover Dataset

At the time of writing, no ground-based cloud monitoring data were available that explicitly addressed multi-GEO, multi-OGS scenarios. Consequently, we adapt our existing cloud coverage data, initially collected from a single OGS and reported in [5] and [18], for application to this study.

Images are collected by an ASI at the Plataforma Solar de Almería (PSA), a facility of the Spanish Centre for Energy, Environmental and Technological Research (CIEMAT), where an OGS from German Aerospace Center (DLR) is currently under construction. Clouds in these images are then segmented using a deep learning approach, achieving pixel-wise accuracy of 95 % [17]. The important characteristics of the dataset are detailed in TABLE I.

TABLE I
SUMMARY OF KEY PROPERTIES OF THE ORIGINAL DATASET

Number of samples in original dataset	984 819
Beginning of recording	1st of August 2019
End of recording	31st of August 2021
Sampling period	30 s
Image resolution	512 × 512 pixels
Probability of visibility along each LOS path	66.89 %
Median duration of visible intervals	1.5 to 2 min
Median duration of cloud-covered intervals	1.5 to 2 min
Number of OGSs in new dataset	9
Number of data samples for each OGS	80 000

The correlation matrix between the visibility on LOS paths from the satellites to each OGS, represented by binary time series, is shown in Fig. 3. We arbitrarily selected 9 positions for GEO satellites, equally distributed along the GEO arch for model simplicity. The satellites are separated by 20° in longitude to provide a certain degree of diversity between paths, while the elevation of the lowest satellite is set to 10°. This elevation approximately defines the lower operational limit for most OGSs to enable reliable FSOC connections. Note that we create a model scenario aiming at proving the concept. When applied to real-world scenarios this needs to be refined with the actual OGS locations and satellite positions.

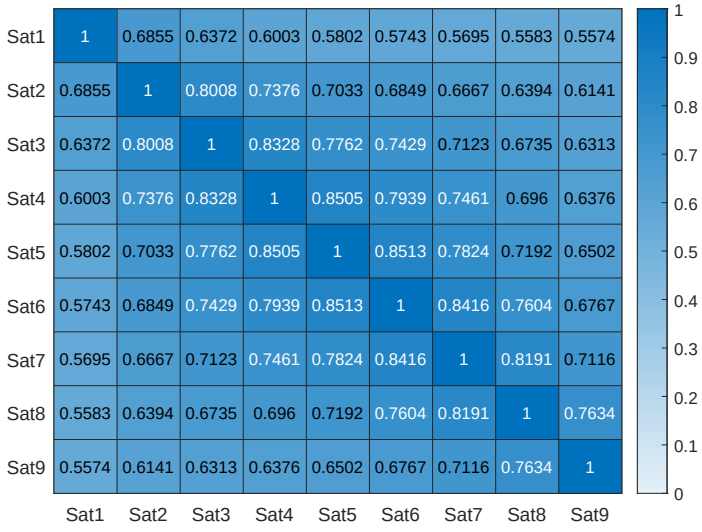

Fig. 3. Correlation matrix illustrating visibility relationships between satellite-to-OGS paths in the original dataset.

Cloud conditions are temporally uncorrelated over several months, as shown in Fig. 4. Therefore, we partitioned the recorded cloud coverage time series into equally sized intervals of at least two months each. Each uncorrelated subseries derived from these intervals was then treated as representative cloud data for an individual OGS, enabling the simulation of simultaneous cloud conditions at up to 12 distinct OGSs using the original two-year-long dataset. Furthermore, the new dataset remains sufficiently long with about 80 000 samples, allowing us to conduct a large number of Monte Carlo simulation runs. The restructuring procedure is illustrated in Fig. 5. It should be noted that this method requires identical long-term cloud coverage probabilities across all OGS sites—an assumption that may not always hold in practice. Nonetheless, the resulting synthetic dataset provides a statistically consistent and reliable basis for simulating multi-GEO, multi-OGS networks, while preserving the temporal and statistical characteristics of real-world visibility data.

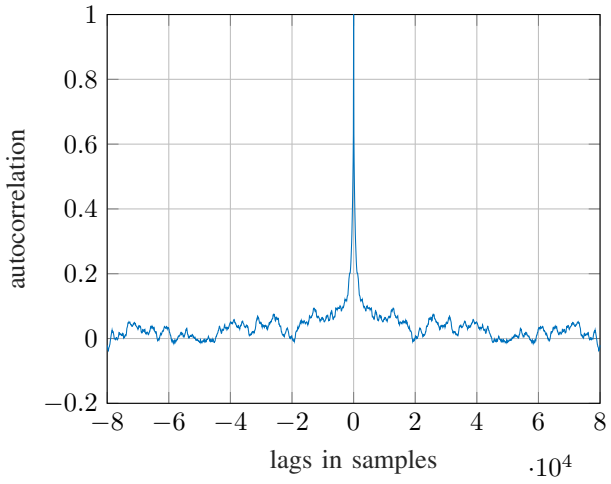

Fig. 4. Autocorrelation of a visibility time series from an OGS to a satellite. The maximum lag corresponds to roughly two months of data. The autocorrelation decreases to near zero for lags longer than half a month, confirming that cloud coverage conditions can be considered statistically independent beyond such time intervals.

III. GROUND-TO-GEO NETWORK PERFORMANCE

We employ average capacity and outage probability as two metrics to evaluate the network performance, providing a comprehensive assessment of the system behavior under varying cloud coverage conditions.

A. Statistical Model of Network Throughput

In this subsection, we present a statistical analysis of the maximum number of simultaneous connections (maxflow) in OFL networks. For a given visibility matrix $\mathbf{V}_i$, the maximum network throughput can be derived as follows

$$\mathcal{C}(\mathbf{V}_i) = \text{maxflow}(\mathbf{V}_i) \cdot \mathcal{C}_0, \tag{2}$$

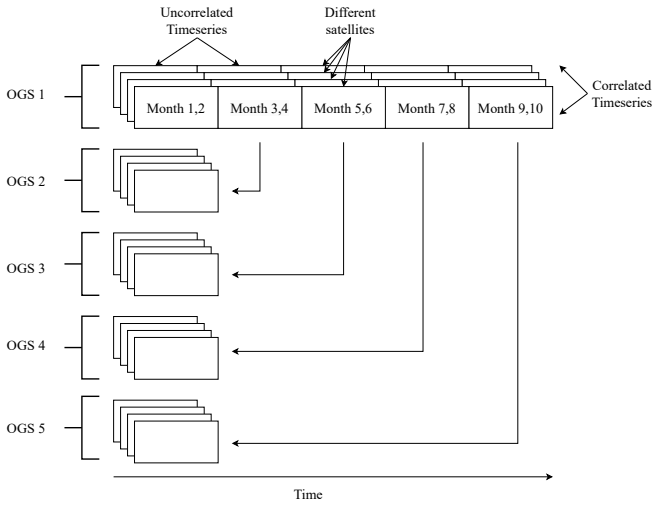

Fig. 5. Restructuring of cloud observation data from a single OGS into parallel, uncorrelated time series used to simulate the multi-GEO, multi-OGS scenario.

where maxflow($\mathbf{V}_i$) denotes the number of vertex-disjoint paths in the graph, corresponding to the maximum number of OFLs as introduced in Subsection II-A, and $\mathcal{C}_0$ is the data rate of a single link between a satellite OGS pair. The average network capacity can then be calculated as

$$\begin{aligned}\mathbb{E}[\mathcal{C}] &= \frac{1}{|\Omega|}\sum_{\mathbf{V}_i}\mathcal{C}(\mathbf{V}_i)P(\mathbf{V}_i)\\ &= \frac{1}{|\Omega|}\sum_{\mathbf{V}_i}\text{maxflow}(\mathbf{V}_i)\cdot\mathcal{C}_0 P(\mathbf{V}_i),\end{aligned} \tag{3}$$

where $|\Omega|$ is the number of all possible outcomes of $\mathbf{V}_i$ and $P(\mathbf{V}_i)$ is the probability of the visibility matrix $\mathbf{V}_i$. Furthermore, the probability of the visibility matrix $P(\mathbf{V}_i)$ can be calculated from the cloud coverage probability of each LOS propagation path as follows:

$$P(\mathbf{V}_i) = \prod_{m=1}^{M}\prod_{n=1}^{N} P(v_{mn}), \tag{4}$$

assuming that the visibility v_{mn} on different paths is statistically independent. However, as mentioned in the previous section, the visibilities from a single OGS to satellites within its FOR, presented by elements in the same matrix row, are correlated. The calculation in (4) must , therefore, be refined to

$$P(\mathbf{V}_i) = \prod_{m=1}^{M} P(v_{m1}, v_{m2}, ...v_{mN}), \tag{5}$$

where $P(v_{m1}, v_{m2}, ...v_{mN})$ denotes the joint probability of N dependent random variables (RVs) representing visibilities of the m-th OGS to all satellites. Trying to determine this joint probability for each OGS is not practical, as the number of possible visibility matrix $\mathbf{V}_i$ is 2^{NM}, which is exponential to the number of satellites and OGSs. Therefore, calculating the exact capacity of the network is extremely computationally expensive even for a small number of satellites and OGSs.

To simplify the analysis, we estimate the average capacity via Monte Carlo simulations. The simulation procedure is as follows: initially, we generate a visibility matrix using binary RVs or select a visibility matrix in the modified dataset in Subsection II-B. Next, we determine the maximum number of available connections through the max-flow algorithm. Finally, we calculate the average network capacity (average maxflow) by aggregating results from multiple simulation runs. This approach yields a reliable estimate of the mean network capacity despite the statistical dependence of the matrix realizations, as we assume that the matrix elements follow an identical distribution for simplification.

B. Network Outage Probability

The network outage probability is defined as the probability that the network fails to establish any satellite-to-OGS connections. It is expressed as

$$P_{\text{out}} = P(v = \mathbb{O}), \tag{6}$$

where $\mathbb{O}$ denotes the zero matrix. When the visibility v_{mn} of different OGS sites is statistically independent, the network outage probability can be expressed as the product of cloud coverage probabilities along each LOS propagation path:

$$P_{\text{out}} = \prod_{m=1}^{M} P\left(\prod_{n=1}^{N} v_{mn} = 0\right), \tag{7}$$

where $P\left(\prod_{n=1}^{N} v_{mn} = 0\right)$ represents the joint probability that the m-th OGS is simultaneously unable to establish visibility with any satellite.

In practice, OGSs are strategically located in regions with statistically favorable weather conditions to ensure a consistently high probability of satellite visibility—typically above $60\,\%$. $60\,\%$ In our simulation, to investigate system behavior under a range of scenarios—including arbitrary link outage probabilities and different degrees of visibility correlation not captured by the measured dataset— correlated binary RVs are employed. These random variables are generated using the method of conditional probabilities, ensuring a controlled degree of pairwise correlation between visibility states.

IV. Simulation Results and Discussion

In this section, we present the maximum flow and outage probability of the proposed OFL network model. The simulation parameters, including annual mean cloud coverage and the correlation of the visibility of the satellites to the same OGS, are varied to study their impact on network capacity. The measurement results in [17] are used as reference values for parameter selection.

A. Impact of Visibility Correlation on Network Capacity and Reliability

Figure 6 illustrates the average maximum number of OFL connections (maxflow) for a configuration comprising two GEO satellites. The annual mean probability of clear sky of all LOS links is set to be 66 %, equal to the average value in our dataset. The lines correspond to different visibility correlations ρ from each OGS to the two satellites. The results show that as the number of OGSs increases, the average maximum number of OFL connections (maxflow) also increases. However, the increase is not linear, as the number of connections is limited by the number of satellites. All lines reach their maximum available flow $\mathcal{C}/\mathcal{C}_0 = 2$ by $M = 5$ OGSs. Moreover, when the visibility conditions for different satellites at the same OGS are less correlated, the network capacity is also higher. Even though the differences between the correlation levels are relatively small, the trend remains consistent across all scenarios.

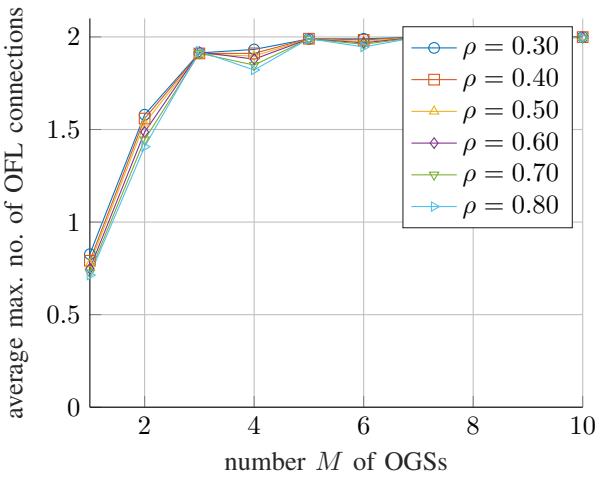

Fig. 6. Average maximum number of OFL connections (maxflow) for different values of the visibility correlation ρ in a network with $N = 2$ GEO satellites.

The influence of the visibility correlation on the probability of network outages is depicted in Fig. 7.. The results indicate that the outage probability decreases with an increasing number of OGSs. Furthermore, the outage probability is lower when the visibility conditions for different satellites at the same OGS are less correlated. In [17], the visibility correlation between two GEO satellites separated by 20° is $\rho = 0.8$. In this case, the system availability of 99.98 % is achieved by $M = 7$ OGSs. If the correlation could be reduced to $\rho = 0.5$ by a larger angular spacing of the GEO satellites, the number of required OGS could be reduced to $M = 6$. In this scenario, i.e., with $M = 2$, the maximal capacity $\mathcal{C}/\mathcal{C}_0 = 2$ and an acceptable system availability can be achieved, while keeping the number of OGSs small.

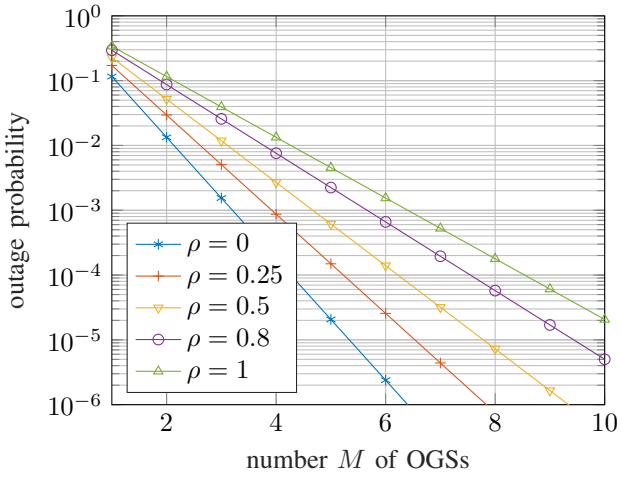

Fig. 7. Outage probability for different visibility correlation values ρ in an $N = 2$ GEO satellite network. Here, $\rho = 1$ corresponds to the case in which only a single satellite is effectively visible.

B. Network Capacity in Multi-GEO Multi-OGS Networks

In the next simulation, we consider the GEO-to-ground OFL network with up to 9 GEO satellites and 12 OGSs. The data used in this simulation are modified from the dataset from our last measurement as described in Subsection II-B. We perform 80 000 simulation trials for each network design in MATLAB.

Fig. 8 presents the average maxflow for varying numbers of satellites and OGSs. Across all configurations, a similar trend is observed: the average maxflow increases with the number of OGSs, but begins to saturate once their number exceeds that of the satellites. Despite the strong correlation in LOS visibility and the high likelihood of link outages, the maxflow approaches its theoretical maximum of $\min(N, M)$ even when only $N + 1$ OGSs are used. This suggests that in a OFL network with a fixed number of GEO satellites N, only a small number of additional or even a single redundant OGS is required to achieve the maximum available network capacity $\mathcal{C}/\mathcal{C}_0 = N$. In contrast, in a network with 15 OGSs suggested by European Space Agency (ESA) [26], 16 represents the optimal number of GEO satellites required to fully exploit the available ground-segment capacity.

V. Conclusion and Outlook

In this study, we have proposed an optical ground-to-GEO network model, where GEO satellites are connected to OGSs by OFLs. Cloud obstruction has been assumed to constitute the dominant constraint on network performance. We first formulate the network capacity as a maximum flow problem, which can be addressed using existing maximum flow algorithms. We then evaluate the network capacity and availability across different scenarios, varying the strengths of visibility correlation and the number of communication nodes (OGSs and GEO satellites). Synthetic timeseries and a modified real-world cloud dataset are employed for the simulations. The results

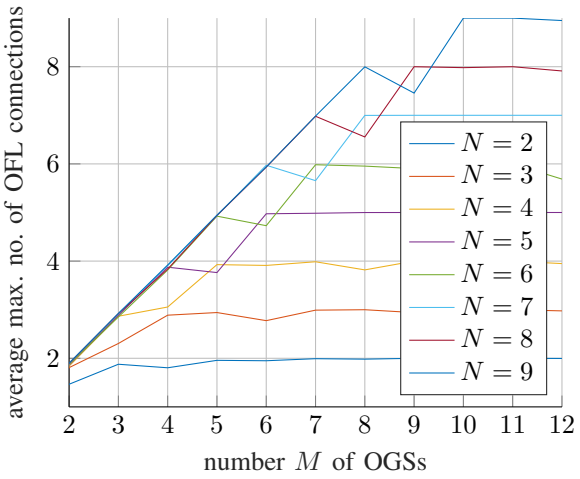

Fig. 8. Average maximum number of connections by various number of communication nodes, with N as number of satellites in GEO orbit.

show that while visibility correlation significantly increases the probability of network outages, its influence on overall network capacity is negligible when maxflow-based network planning is applied. Furthermore, the results indicate that despite the high measured outage probability and strong visibility correlation observed in the data, the network capacity can be maximized with only a small number of additional OGSs. These findings provide practical guidelines for determining the optimal number of GEO satellites and OGSs to achieve high-capacity and resilient optical networks.

Future work will focus on refining and extending the network model to incorporate additional atmospheric factors and dynamic link characteristics. With advances in cloud monitoring technology, the visibility of satellites to OGSs can be detected, classified, and forecasted in real time. Different types of clouds, depending on their altitude and thickness, may cause varying levels of signal attenuation, leading to partial reductions in data rates. Furthermore, free-space losses and atmospheric attenuation can be influenced by OFL elevation or satellite motion in cases of LEO constellations, such as Starlink or OneWeb. These degradations (but not disruptions) of link capacity can be represented by fractional values in the visibility matrix. Incorporating these factors will enable a more accurate link budget estimation and broaden the applicability of the proposed approach, although this also requires more complex climatological monitoring systems. Accordingly, the proposed maxflow-based planning framework will be extended to fractional-capacity network models to support more adaptive and resilient future optical networks.

As part of current satellite payloads as well as ongoing research , multi-aperture (point-to-multipoint) optical terminals for GEO satellites are being developed [27]–[29]. Using these terminals, feeder links can be established from a single GEO satellite to multiple OGSs. The network capacity of such point-to-multipoint systems can be evaluated using a modified version of the maxflow approach introduced in this paper, where the connection from the source s to each satellite node in Fig. 2 is assigned a flow equal to the number of apertures installed at the DTE optical terminal. The cost-performance trade-off of these advanced systems will be analyzed in future studies.

ACKNOWLEDGMENT

This research work is funded by dtec.bw—Digitalization and Technology Research Center of the Bundeswehr. Dtec.bw is funded by the European Union – NextGenerationEU.

REFERENCES

[1] F. C. Commission, "Application for Modification – SAT-MOD-20200417-00037," 2020. [Online]. Available: https://fcc.report/IBFS/SAT-MOD-20200417-00037

[2] N. J. Rattenbury, J. Ashby, F. Bennet, M. Birch, J. E. Cater, K. Ferguson, D. Giggenbach, K. Grant, A. Knopp, M. T. Knopp *et al.*, "Update on the German and Australasian optical ground station networks," *arXiv preprint arXiv:2402.13282*, 2024.

[3] W. Roberts, D. Antsos, A. Croonquist, S. Piazzolla, L. Roberts Jr, V. Garkanian, T. Trinh, M. Wright, R. Rogalin, J. Wu *et al.*, "Overview of Ground Station 1 of the NASA Space Communications and Navigation Program," in *Free-Space Laser Communication and Atmospheric Propagation XXVIII*, vol. 9739. SPIE, 2016, pp. 82–99.

[4] S. Piazzolla, W. T. Roberts, J. Kovalik, M. Peng, V. Garkanian, C. Chen, W. Buehlman, M. Brewer, G. Ortiz, K. Matthews *et al.*, "Ground station for Terabyte Infrared Delivery (TBIRD)," in *Free-space laser communications XXXV*, vol. 12413. SPIE, 2023, pp. 280–295.

[5] H. Le Son, R. T. Schwarz, M. T. Knopp, D. Giggenbach, and A. Knopp, "Optical feeder links to GEO satellites: Statistical analysis of link availability using deep learning-based cloud segmentation data," in *2025 IEEE International Conference on Communications (ICC)*, 2025.

[6] R. Link, M. E. Craddock, and R. J. Alliss, "Mitigating the impact of clouds on optical communications," in *2005 IEEE Aerospace Conference*. IEEE, 2005, pp. 1258–1265.

[7] G. S. Wojcik, H. L. Szymczak, R. J. Alliss, R. P. Link, M. E. Craddock, and M. L. Mason, "Deep-space to ground laser communications in a cloudy world," in *Free-Space Laser Communications V*, vol. 5892. SPIE, 2005, pp. 17–27.

[8] A. Benarroch, P. G. Del Pino, and J. Riera, "Spatial properties of cloud cover and rainfall rate based on data from Spanish sites," in *2006 First European Conference on Antennas and Propagation*. IEEE, 2006, pp. 1–8.

[9] P. Garcia, A. Benarroch, and J. M. Riera, "Spatial distribution of cloud cover," *International Journal of Satellite Communications and Networking*, vol. 26, no. 2, pp. 141–155, 2008.

[10] F. Moll and M. Knapek, "Wavelength selection criteria and link availability due to cloud coverage statistics and attenuation affecting satellite, aerial, and downlink scenarios," in *Free-Space Laser Communications VII*, vol. 6709. SPIE, 2007, pp. 347–358.

[11] F. Lacoste, A. Guérin, A. Laurens, G. Azema, C. Periard, and D. Grimal, "FSO ground network optimization and analysis considering the influence of clouds," in *Proceedings of the 5th European Conference on Antennas and Propagation (EUCAP)*, 2011, pp. 2746–2750.

[12] C. Fuchs and F. Moll, "Ground station network optimization for space-to-ground optical communication links," *Journal of Optical Communications and Networking*, vol. 7, no. 12, pp. 1148–1159, 2015.

[13] C. Fuchs, S. Poulenard, N. Perlot, J. Riedi, and J. Perdigues, "Optimization and throughput estimation of optical ground networks for LEO-downlinks, GEO-feeder links and GEO-relays," in *Free-Space Laser Communication and Atmospheric Propagation XXIX*, vol. 10096. SPIE, 2017, pp. 298–307.

[14] S. Poulenard, M. Crosnier, and A. Rissons, "Ground segment design for broadband geostationary satellite with optical feeder link," *Journal of Optical Communications and Networking*, vol. 7, no. 4, pp. 325–336, 2015.

[15] S. Sunil, B. Padmakumari, G. Pandithurai, R. D. Patil, and C. Naidu, "Diurnal (24 h) cycle and seasonal variability of cloud fraction retrieved from a Whole Sky Imager over a complex terrain in the Western Ghats and comparison with MODIS," *Atmospheric Research*, vol. 248, p. 105180, 2021.

[16] D. Kolev, A. Carrasco-Casado, K. Suzuki, and M. Toyoshima, "Environmental-data collection system testbed for site-diversity implementation in satellite-to-ground laser communications," in *2017 IEEE International Conference on Space Optical Systems and Applications (ICSOS)*. IEEE, 2017, pp. 286–289.

[17] Y. Fabel, B. Nouri, S. Wilbert, N. Blum, R. Triebel, M. Hasenbalg, P. Kuhn, L. F. Zarzalejo, and R. Pitz-Paal, "Applying self-supervised learning for semantic cloud segmentation of all-sky images," *Atmospheric Measurement Techniques*, vol. 15, no. 3, pp. 797–809, 2022.

[18] M. T. Knopp, D. Giggenbach, M. Giggenbach, and B. Nouri, "Assessment of CIEMAT's Plataforma Solar de Almeria as a ground station site for optical LEO satellite downlinks," in *International Conference on Space Optics—ICSO*, 2024.

[19] A. Fürbacher, T. Fruth, A. Wiebigke, M. T. Wörle, F. Mrowka, K. Saucke, P. Martín Pimentel, and M. Knopp, "Concept for generic agile, reactive optical link planning," *CEAS Space Journal*, pp. 1–10, Jan. 2025. [Online]. Available: https://link.springer.com/10.1007/s12567-025-00592-0

[20] Y. Liu, X. Li, D. Li, L. Zhang, and S. Huang, "Free-space optical (FSO) feeder link planning in space-ground integrated optical networks (SGIONs): Trade off throughput and dynamics," *Optics Express*, vol. 31, no. 21, pp. 35 396–35 418, 2023.

[21] K. M. Riesing, C. M. Schieler, J. S. Chang, N. J. Gilbert, A. J. Horvath, R. S. Reeve, B. S. Robinson, J. P. Wang, P. S. Agrawal, and R. A. Goodloe, "On-orbit results of pointing, acquisition, and tracking for the TBIRD CubeSat mission," in *Free-Space Laser Communications XXXV*, vol. 12413. SPIE, 2023, pp. 25–33.

[22] F. Lin, Y. Zhang, and J. Wang, "Recent advances in intra-hour solar forecasting: A review of ground-based sky image methods," *International Journal of Forecasting*, vol. 39, no. 1, pp. 244–265, 2023.

[23] B. Nouri, Y. Fabel, N. Blum, D. Schnaus, L. F. Zarzalejo, A. Kazantzidis, and S. Wilbert, "Ramp rate metric suitable for solar forecasting," *Solar RRL*, vol. 8, no. 24, p. 2400468, 2024.

[24] D. Giggenbach, M. T. Knopp, and C. Fuchs, "Link budget calculation in optical LEO satellite downlinks with on/off-keying and large signal divergence: A simplified methodology," *International Journal of Satellite Communications and Networking*, vol. 41, no. 5, pp. 460–476, 2023.

[25] Y. Boykov and V. Kolmogorov, "An experimental comparison of min-cut/max-flow algorithms for energy minimization in vision," *IEEE transactions on pattern analysis and machine intelligence*, vol. 26, no. 9, pp. 1124–1137, 2004.

[26] Z. Sodnik, C. Voland, J. Perdigues, E. Fischer, K. Kudielka, and R. Czichy, "Optical feeder-link between ESA's optical ground station and Alphasat," in *International Conference on Space Optics—ICSO 2020*, vol. 11852. SPIE, 2021, pp. 520–526.

[27] A. Hylton, D. Israel, and M. Palsson, "Laser communications relay demonstration: experiments with delay tolerant networking," in *40th International Communications Satellite Systems Conference (ICSSC 2023)*, vol. 2023, 2023, pp. 106–111.

[28] J. Poliak, D. Blandino, M. Albertini, M. Beier, M. Hornaff, S. Raffa, R. M. Calvo, Z. Sodnik, and A. Jones, "Multiple optical receive system for a single optical terminal: Preliminary design," in *Free-Space Laser Communications XXXIV*. SPIE, 2022, p. PC1199304.

[29] J. Poliak, M. Albertini, M. Beier, G. Cilia, M. Hornaff, M. Marmonti, L. Reger, M. Schulz, and A. Urbich, "Multiple optical receive system for optical GEO feeder-links," in *Free-Space Laser Communications XXXVI*, vol. 12877. SPIE, 2024, pp. 203–211.

Robert T. Schwarz (Member, IEEE) received his Ph.D. degree (Hons.) in satellite communications from the University of the Bundeswehr Munich in 2019. From 2006 to 2012, he was with the Federal Office of Bundeswehr Equipment, Information Technology and In-Service Support, where he was involved in the German Program for Satellite Communications of the Bundeswehr (SATCOMBw). Since 2012, he has been a Research Fellow at the University of the Bundeswehr Munich. His research interests include digital signal processing, waveform design, and MIMO for satellites and other non-terrestrial networks. He is a member of the German Engineers' Association, VDE / ITG, and AFCEA.

Hung. Le Son received his bachelor's and master's degrees in Electrical Engineering and Information Technology from the University of the Bundeswehr Munich in 2020 and 2021. Since 2021, he has been a research fellow with the Department of Electrical Power Systems and Information Technology at the University of the Bundeswehr in Munich, Germany. His research interests include diversity approaches to enhance system availability in free-space optical communications.

Marcus T. Knopp received his Ph.D. in natural sciences from the Ludwig-Maximilians-University Munich in 2014 focusing on optical methods and their application in scientific and technical environments. With his move to the German Aerospace Center (DLR) in 2015, he entered the field of laser-based satellite communications. Since 2022 he is heading the Ground Segment Department of DLR's Responsive Space Cluster Competence Center. In addition, he has been a lecturer at the University of the Bundeswehr in Munich for several years. His research interest is in the utilization of free-space optical communications for operational data-relay applications. Currently, his work is centered upon the development of robotic optical ground stations and the investigation of link optimization strategies.

Andreas Knopp (Senior Member, IEEE) received the Ph.D. degree (Hons.) in radio communications from the University of the Bundeswehr Munich in 2008. Since 2014, he has been a Full Professor of signal processing and has also coordinated the Munich Center for Space Communications, which is Germany's largest SpaceCom Laboratory and Experimental Satellite Ground Station. Before taking up a faculty position, he gained expertise as a Communications Engineer and the Satellite Program Manager. His current research interests include satellite network integration and waveform design for 6G, digital satellite payloads, secure/antijam communications, and low-power mMTC. He is an Entrepreneur and the Co-Founder of two start-up companies that have implemented his research. He is an advisor to the German MoD and a member of the Expert Group on Radio Systems, German Engineers' Association, VDE/ITG, and AFCEA.